

# Field emission current cleaning and annealing of microfabricated cold cathodes

P. R. Schwoebel,<sup>a)</sup> C. A. Spindt, and C. E. Holland  
*Applied Physical Sciences Laboratory, SRI International, Menlo Park, California 94025*

J. A. Panitz  
*Department of Physics and Astronomy, University of New Mexico, Albuquerque, New Mexico 87131*

(Received 6 October 2000; accepted 18 December 2000)

Thermal cleaning and annealing by the extracted field emission current has been used to achieve and maintain stable emission characteristics with microfabricated cold field emission cathodes. Our studies show that the cathode tip surface can be smoothed, recrystallized, and at least partially cleaned of surface adsorbates. The result is a significant decrease in emission current noise and recovery of the initial current–voltage characteristics of the cathode following surface contamination. © 2001 American Vacuum Society. [DOI: 10.1116/1.1349206]

## I. INTRODUCTION

The surface structure and chemical composition of microfabricated field emitter tips govern the current–voltage ( $I$ – $V$ ) characteristics by defining the electron tunneling barrier. These field emitter tips are typically composed of emitting surfaces having a structure that exhibits few signs of crystallinity and a chemical composition that is essentially unknown.<sup>1</sup> Adsorption of common contaminants on the emitting surface will increase the average work function and the emission current noise.<sup>2</sup>

To date, the most successful commercial application of cold field emission has been as electron sources in high resolution electron microscopes.<sup>3</sup> The  $I$ – $V$  characteristics and emission current stability of the etched wire tips used for this purpose are maintained by thermal treatment with joule heating of the hairpin filament to which the tip is attached. This treatment results in thermal desorption of surface contaminants that gradually adsorb on the tip surface from the residual gas atmosphere within the microscope. The tip heating is also sufficient to initiate surface self-diffusion which mitigates the effects of ion bombardment induced surface roughening and sputtering. Without thermal treatment, adsorption changes the average  $I$ – $V$  characteristics with time and increases emission current noise,<sup>2</sup> and surface roughening and sputtering by ion bombardment leads to the eventual initiation of a vacuum arc and destruction of the emitter tip.<sup>2,4</sup> The effects of ion bombardment are greatly suppressed with microfabricated emitter tips<sup>5</sup> due to the presence of the gate electrode, which helps to electrostatically shield the tip from bombardment by energetic ions formed in the gate–anode gap.

The following operational problems have been identified in field emitter array based device development efforts: (1) a roughly monotonic decrease with time of the mean emission current at constant applied voltage and (2) fluctuations of the emission current at a constant voltage about this decreasing mean. The results of these operational problems are poor

time correlation between the applied voltage and emitted current and the need to gradually increase the applied voltage to maintain a given current.

Typically, adsorption on the tip surface leads to a monotonic decrease in emission current with time at constant voltage. Surface contaminants, whether by adsorption, desorption, or unstable residence on the tip surface,<sup>6</sup> can induce emission current fluctuations. Because such phenomena are statistical processes, the ratio of the magnitude of the emission current fluctuations to the total current varies inversely as the square root of the tip surface emitting area.<sup>7</sup> To achieve emission current stability, one must maintain a clean tip surface and maximize the emitting area.

Earlier, we presented the initial results of microfabricated single tip self-heating by pulsing the field emission current to levels of approximately 200  $\mu$ A, at which the onset of surface adsorbate removal was observed.<sup>8</sup> The mechanism of adsorbate removal is believed to be thermal desorption due to heating of the tip by the extracted electron current. In these previous experiments, higher pulsed emission current levels were not reliably achieved due to voltage breakdown across or through the insulator ( $\sim 0.6 \mu$ m thermal SiO<sub>2</sub>), separating the base and gate electrodes of the cathode. We recently used a procedure<sup>9</sup> by which cathodes having a high aspect ratio can be grown with an insulating oxide thickness of  $\sim 1.5 \mu$ m. This allows for the application of higher voltages to the cathode and the extraction of significantly higher currents for a given tip radius and shape. This article reports the results of *in situ* cleaning and annealing of microfabricated emitter tip surfaces using these cathodes.

## II. EXPERIMENT

The experimental chamber was a metal field emission microscope operating at a base pressure below  $10^{-10}$  Torr following a 12 h system bakeout at 200 °C. The cathodes were Spindt-type molybdenum single-tip emitters mounted on T0-5 headers. During cathode operation, the gate electrode current was always below the 10 nA detectable level for our arrangement. Square-wave 100  $\mu$ s negative voltage pulses

<sup>a)</sup>Electronic mail: pauls@chtm.unm.edu

were applied to the tip relative to a grounded gate electrode at a frequency of 5 Hz. The time for which the cathode is operated in the pulsed mode  $t_{on}$  is the duty cycle multiplied by the total elapsed time. The emission current pulses were capacitively coupled from the phosphor anode (maintained at 2–3 kV), passed through a transimpedance amplifier, and viewed on a Tektronix 540D oscilloscope. The pulsed emission current tracked the shape of the input voltage pulse wave form (rise rate of 0.25 V/ns), demonstrating reasonable impedance matching. During current pulsing capacitive coupling between the gate and base electrodes negated the measurement of current, if any, that impinged on the gate electrode. Field emission images were recorded on phosphor screens ( $P-I$ ) using 35 mm or 4×5 in. Polaroid black/white film. The  $f$  stop or exposure time was adjusted to enhance important details in the emission images so there is not a direct correlation between image brightness and electron current density in the micrographs. Fowler–Nordheim (FN) plots of  $I-V$  data reference the intercept and slope,  $\ln a$  and  $b$  respectively, given by the FN equation

$$I = aV^2 e^{(-b/V)},$$

where  $I$  is the emission current and  $V$  the applied voltage. The emitting area  $A_e$  was calculated using the equation<sup>5</sup>

$$A_e = kab^2,$$

where  $k$  is a constant.

### III. RESULTS AND DISCUSSION

#### A. $I-V$ characteristics

Two distinct phenomena were observed in the cathode's  $I-V$  characteristics. First, at pulsed current levels of approximately 200  $\mu A$  a reversible change occurs that we attribute to the thermal desorption and subsequent readsorption of surface contaminants arriving from the gas phase.<sup>8</sup> Second, at pulsed current levels greater than approximately 1 mA, an irreversible change occurs that can be attributed to a permanent modification of the tips' geometrical structure by field-assisted thermally activated surface self-diffusion.<sup>10</sup>

Curve A in Fig. 1 shows the FN plot of a single as-fabricated molybdenum Spindt tip following 72 h of operation at 10  $\mu A$  emission current in  $5 \times 10^{-11}$  Torr. Curve B in Figs. 1 and 2 is the result of pulsed operation of the cathode at 200  $\mu A$  for 5 min (equivalent to a total on time  $t_{on}$  of 0.15 s). The current for a given voltage increased with an associated increase in emitting area and decrease in FN slope. Similar changes were observed for 25 different cathodes under the same pulsing conditions with the current varying from  $\sim 150$  to 400  $\mu A$ .

The  $I-V$  characteristic shown in curve B gradually reverts to that shown in curve A during operation for several hours at emission levels of several  $\mu A$ s. The change in the  $I-V$  characteristic between prepulsing (curve A) and post-pulsing (curve B) is reproducible. Because the process is reversible, no change in tip geometry has occurred. We associate changes between prepulsing and postpulsing  $I-V$  data with the adsorption and thermal desorption of residual

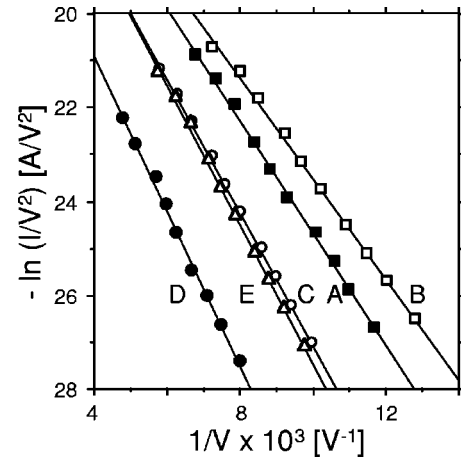


FIG. 1. Fowler–Nordheim data showing the changes associated with emission current pulsing of a single tip cathode. Curve A: As-fabricated tip (FN parameters:  $a = 3.05 \times 10^{-6} [A/V^2]$ ,  $b = -1200 [V]$ ). Curve B: Following emission current pulsing at 200  $\mu A$  ( $a = 3.26 \times 10^{-5} [A/V^2]$ ,  $b = -1070 [V]$ ). Curve C: Following emission current pulsing at 700  $\mu A$  ( $a = 2.50 \times 10^{-6} [A/V^2]$ ,  $b = -1420 [V]$ ). Curve D: Following cathode operation for 12 h at 10  $\mu A$  ( $a = 6.16 \times 10^{-7} [A/V^2]$ ,  $b = -1650 [V]$ ). Curve E: Following emission current pulsing at 200–300  $\mu A$  ( $a = 4.55 \times 10^{-6} [A/V^2]$ ,  $b = -1490 [V]$ ). Cathode No. 39J-514F-40B.

gas (probably hydrogen) from the cathode surface which, respectively, increases and decreases the average work function of the emitter apex.

Similar, but not identical, changes were obtained whether or not the cathode was operated during recontamination from the gas phase. In either case, emission current pulsing could be used to recover the  $I-V$  characteristics observed prior to cathode contamination. We tentatively conclude from our observations that the results of recontamination result in an effectively higher work function for a given time and pressure if the cathode is operated during the recontamination process.

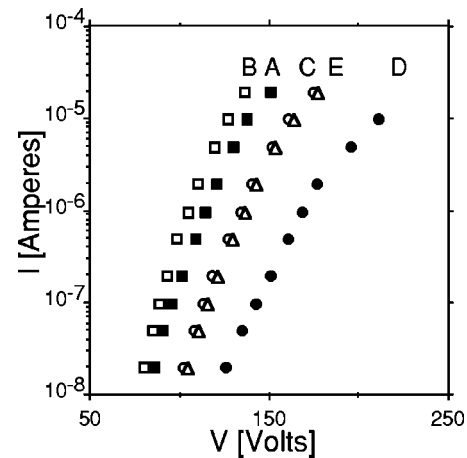


FIG. 2.  $I-V$  data for the FN plots shown in Fig. 1. Curve A: As-fabricated tip. Curve B: Following emission current pulsing at 200  $\mu A$ . Curve C: Following emission current pulsing at 700  $\mu A$ . Curve D: Following cathode operation for 12 h at 10  $\mu A$ . Curve E: Following emission current pulsing at 200–300  $\mu A$ .

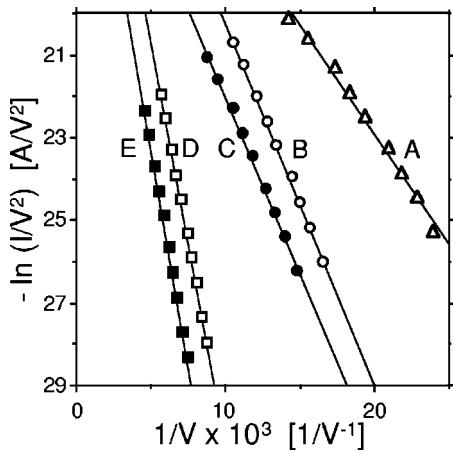


FIG. 3. Fowler–Nordheim data showing the changes associated with emission current pulsing of a single tip cathode. Curve A: As-fabricated tip ( $a = 4.43 \times 10^{-6} [\text{A}/\text{V}^2]$ ,  $b = -530 [\text{V}]$ ). Curve B: Following emission current pulsing at  $400 \mu\text{A}$  ( $a = 1.08 \times 10^{-5} [\text{A}/\text{V}^2]$ ,  $b = -879 [\text{V}]$ ). Curve C: Following operation for 5 h at  $1 \mu\text{A}$  ( $a = 1.35 \times 10^{-6} [\text{A}/\text{V}^2]$ ,  $b = -852 [\text{V}]$ ). Curve D: Following emission current pulsing at  $3.5 \text{ mA}$  ( $a = 1.53 \times 10^{-5} [\text{A}/\text{V}^2]$ ,  $b = -1943 [\text{V}]$ ). Curve E: Following operation for 10 h at  $10 \mu\text{A}$  ( $a = 2.56 \times 10^{-6} [\text{A}/\text{V}^2]$ ,  $b = -2097 [\text{V}]$ ). Cathode No. 39J +163F-1J.

With further increases in the level of pulsed emission current, irreversible changes in the  $I$ – $V$  characteristic could be induced. As an example, consider curve C in Fig. 1 which is a FN plot of the  $I$ – $V$  characteristic after 1 h of current pulsing at  $\sim 700 \mu\text{A}$  ( $t_{\text{on}} = 1.8 \text{ s}$ ). The permanent increase in the voltage required to achieve a given current from the cathode can be attributed to smoothing of the tip surface by thermally activated field assisted surface self-diffusion. At this new level of cathode operation, reversible changes are again observed. During 12 h of operation at an emission level of  $10 \mu\text{A}$ , the  $I$ – $V$  characteristic shifted to that shown in curve D. Subsequent emission current pulsing for 3 min at  $200$ – $300 \mu\text{A}$  ( $t_{\text{on}} = 90 \text{ ms}$ ) essentially restored the  $I$ – $V$  characteristic to that of curve C as shown in curve E. Again, the reversible change in the  $I$ – $V$  characteristic between curves C and D can be attributed to the adsorption of hydrogen on the tip surface. The shift from D to E is likewise attributed to the removal of hydrogen by thermal desorption.

More dramatic changes in the  $I$ – $V$  characteristic due to emission pulsing were also observed, as illustrated by the data shown in Figs. 3 and 4. Curve A shows the characteristic of an as-fabricated emitter tip after 81 h of operation  $10 \mu\text{A}$ . Pulsed operation of the cathode at  $400 \mu\text{A}$  for 6 min ( $t_{\text{on}} = 180 \text{ ms}$ ) induced an irreversible shift in the FN data to curve B. Again, at this new operational level, reversible changes due to adsorption are observed. Here, resuming normal operation resulted in a monotonic decrease in emission current at a given voltage with operational time until a ‘recontaminated’  $I$ – $V$  characteristic is obtained (curve C). In this case the transition from curve B to curve C occurred while operating the tip at  $1 \mu\text{A}$  for 5 h at  $9 \times 10^{-11} \text{ Torr}$ .

For a given pulsed current (cathode temperature), the  $I$ – $V$  characteristic eventually stabilizes, thereby requiring higher pulsed currents to induce further irreversible changes. The

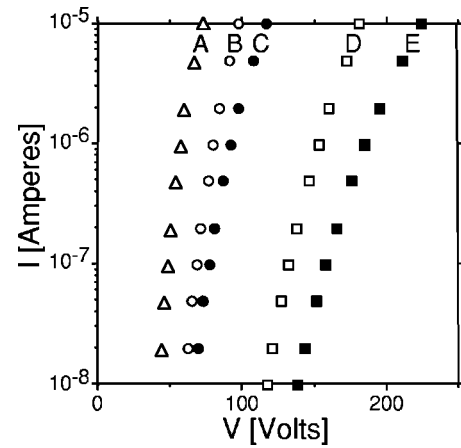


FIG. 4.  $I$ – $V$  data for the FN plots shown in Fig. 3. Curve A: As-fabricated tip. Curve B: Following emission current pulsing at  $400 \mu\text{A}$ . Curve C: Following operation for 5 h at  $1 \mu\text{A}$ . Curve D: Following emission current pulsing at  $3.5 \text{ mA}$ . Curve E: Following operation for 10 h at  $10 \mu\text{A}$ .

highest pulsed current level attempted with this cathode was  $3.5 \text{ mA}$  ( $V_{\text{pulse}} = 345 \text{ V}$ ,  $t_{\text{on}} = 20 \text{ s}$ ). At the cessation of current pulsing, the emission current had decreased to  $2.8 \text{ mA}$  ( $V_{\text{pulse}} = 345 \text{ V}$ ), which had resulted in irreversible cathode operation stabilizing at curve D, Figs. 3 and 4. The FN slope and intercept of curve D predict that the emission current at  $345 \text{ V}$  should be  $\sim 6.5 \text{ mA}$ , indicating that the emission is likely space-charge limited. Curve E is the operational level to which the  $I$ – $V$  characteristic drifts following more normal operation at  $10 \mu\text{A}$  of emission current.

The FN data indicate that the initial emitting area of this tip was equivalent to a circular region only a few atoms in diameter (see curve A, Figs. 3 and 4). This fact is reflected in both the current noise signal, which is proportional to  $1/A_e^{1/2}$ , and the corresponding changes in the electron emission pattern. The cathode showed current fluctuations of  $\pm 30\%$  in its as-fabricated form during operation in a vacuum of  $5 \times 10^{-11} \text{ Torr}$ . Coincident with such large fluctuations, the entire emission pattern was observed to change. The increase in emission area and the removal of adsorbates that yielded curve D in Figs. 3 and 4 resulted in noise levels of less than  $\pm 2\%$ . The emission patterns will be discussed further in the next section.

Pulsing also consistently recovered the cathode’s  $I$ – $V$  characteristics following venting of the vacuum system to laboratory air. Curve A of Fig. 5 shows the  $I$ – $V$  characteristic of the as-fabricated cathode used for Figs. 3 and 4, and curve B the characteristic following pulsing at  $3.5 \text{ mA}$  ( $t_{\text{on}} = 20 \text{ s}$ ). Following accumulation of the  $I$ – $V$  data in curve B, the vacuum chamber was vented directly to laboratory air for 10 min, reevacuated, and baked for 12 h at  $200^\circ\text{C}$ . Curve C shows the  $I$ – $V$  characteristic of the cathode following subsequent operation at an emission current of  $5 \mu\text{A}$  for 24 h. After the emission current was pulsed to  $1.5 \text{ mA}$  ( $t_{\text{on}} = 32 \text{ s}$ ), the  $I$ – $V$  characteristic returned nominally to its pre-venting characteristic, as shown in curve D. Venting of the system to laboratory air followed by a system bakeout after current pulsing typically resulted in a much larger change in

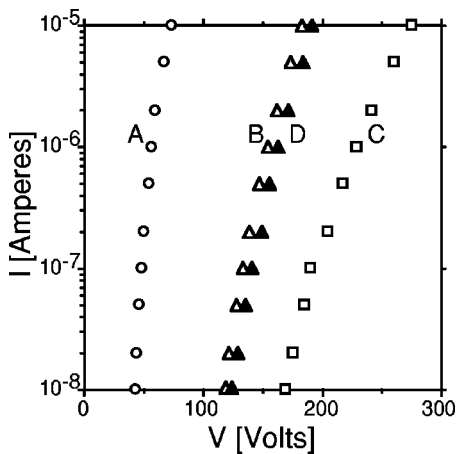


FIG. 5.  $I$ - $V$  characteristics showing the changes associated with venting the vacuum system to laboratory air with a single tip cathode. Curve A: As-fabricated tip. Curve B: Following emission current pulsing at 3.5 mA. Curve C: Following venting, baking, and operation for 24 h at 5  $\mu$ A. Curve D: Following emission current pulsing at 1.5 mA. Cathode No. 39J+163F-1J.

effective tip surface work function than did operation in the vacuum system for several days following current pulsing.

## B. General observations

(1) Current noise of a bistable nature was observed in the extracted current pulse. The relative magnitude of this bistable noise decreased with pulsing time at a given current level in excess of  $\sim 200$   $\mu$ A. This result is consistent with the gradual removal of surface contaminants. During surface cleaning, the current in the extracted pulse could often be observed to increase at a given voltage in discrete steps.

(2) Occasionally, we observed a relatively rapid continual increase in the extracted current at constant voltage during a single pulse. This rise in the current was roughly linear in time, could be on the order of 30%, and was typically seen at emission currents of  $\sim 1$  mA or greater depending on the tip under investigation. The rise is likely due to the removal of surface contamination but could possibly be related to the ‘‘tilt’’ effect,<sup>11</sup> in which tip heating is sufficient to induce significant thermally assisted field emission.

The *reversible* changes in the  $I$ - $V$  characteristics due to emission current pulsing at levels of  $\sim 200$   $\mu$ A and later operation are consistent with the removal of adsorbed residual gas by thermal desorption and its readsorption during cathode operation. Because the changes in the  $I$ - $V$  curves are reversible, no changes in the field-voltage proportionality factor  $\beta$  (i.e., tip shape) occur. This implies that the increase in the slope of the FN plots ( $\propto \phi^{3/2}/\beta$ ) during operation following pulsing is due to an increase in the average work function  $\phi$  of the tip surface. To estimate the minimum observed change in  $\phi$ , we assume that  $\phi$  immediately following pulsing is that of clean polycrystalline molybdenum ( $\phi = 4.3$  eV).<sup>12</sup> Then, for the 25 cathodes investigated, the reversible change in work function ranged with nearly equal probability between 0.1 and 0.5 eV. For reference the aver-

age work function of a conventional etched wire molybdenum tip covered with a chemisorbed layer of hydrogen is 4.9 eV.<sup>13</sup>

The change in emitting area observed during reversible changes in the  $I$ - $V$  characteristics is also consistent with the chemisorption of residual gas during operation and its removal by current pulsing. The emitting area decreased during normal cathode operation after pulsing by factors ranging between 5 and 10. After operation, current pulsing resulted in an increase in emitting area equal to the decrease observed during operation. This change in emitting area is consistent with that observed during the adsorption and thermal desorption of chemically active gases, such as hydrogen and oxygen, from the surface of conventional etched wire emitter tips. With the adsorption of a chemisorbed monolayer of hydrogen on clean tungsten,<sup>14</sup> the emitting area decreases by approximately 10.

The *irreversible* changes in the  $I$ - $V$  characteristics of the cathodes due to emission current pulsing at levels approaching 1 mA are consistent with smoothing of the tip surface by thermally activated field assisted surface self-diffusion of the molybdenum. The resulting decreases in field-voltage proportionality factor  $\beta$  associated with the irreversible increases in voltage required for a given current are reflected by the increases in the slope of the FN plots. Generally, for the 20 cathodes with which this effect was investigated we observed: (1) For  $I \sim 500$   $\mu$ A, the emitting area did not monotonically increase as did the voltage required for a given emission current, and (2) For  $I > 1$  mA, the emitting area monotonically increased with the voltage required for a given current until both stabilized at a given level for a given pulsed emission current. These larger emitting areas (typically 50–500 times greater than that of the as-fabricated cathode) often represented a significant fraction of the maximum emitting area expected with tip radii on the order of 200  $\text{\AA}$ .

The interpretation that reversible changes are due to adsorption and thermal desorption processes and that irreversible changes are associated with surface self-diffusion can also be inferred from plots of the FN parameters  $\ln a$  and  $b$ . A plot of  $\ln a$  vs  $b$  is useful in determining whether changes in the  $I$ - $V$  characteristics are primarily the result of changes in the surface work function, the field-voltage proportionality factor (which is related to the tip radius and shape), or both.<sup>15</sup> This analysis indicates that: (1) Irreversible changes in the  $I$ - $V$  characteristics are due principally to changes in effective tip radius, (2) reversible changes are due to changes in surface work function, and (3) changes from the as-fabricated tip characteristics to the final annealed and at least partially cleaned end form are the result of a decrease in work function and an increase in effective tip radius. Care must be used in interpreting plots of  $\ln a$  vs  $b$  when adsorption results in a change in emitting area. If the change in emitting area is ignored, plots of  $\ln a$  vs  $b$  indicate that a change in work function *and* field-voltage proportionality factor occurred, when there was only a change in work function and emitting area.

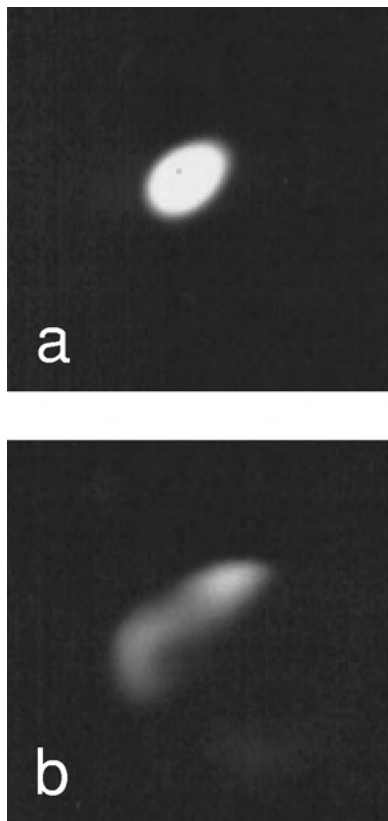


FIG. 6. (a) Pattern of an as-fabricated single tip cathode ( $I=2.0 \mu\text{A}$ ,  $V=116 \text{ V}$ ) and (b) cathode in (a) following an atomic scale surface event ( $I=1.0 \mu\text{A}$ ,  $V=116 \text{ V}$ ). Cathode No. 39J+510F-25C.

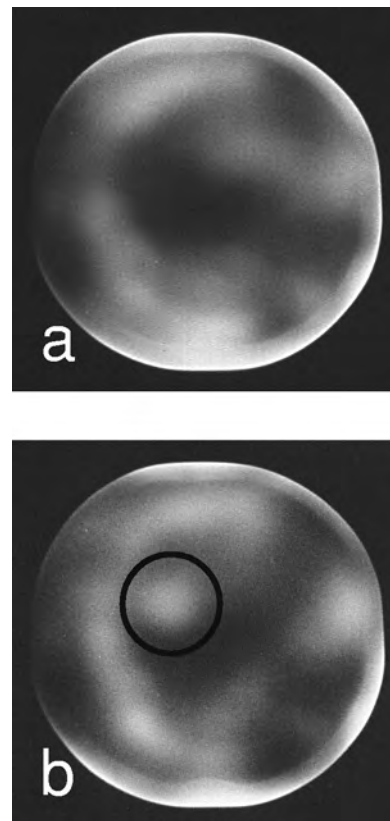


FIG. 7. (a) A single tip cathode following pulsing at 2.2 mA ( $t_{\text{on}}=3 \text{ s}$ ) ( $I=1.5 \mu\text{A}$ ,  $V=150 \text{ V}$ ) and (b) cathode in (a) following an atomic scale surface event ( $I=1.55 \mu\text{A}$ ,  $V=150 \text{ V}$ ). Cathode No. 39J-505F-7R.

### C. Field electron emission patterns

The effects of current pulsing on the emitter tip surface are further clarified by surface imaging studies using the field electron emission microscope (FEEM). FEEM images of the cathodes before and after pulsed current treatment showed two distinct changes in the emission pattern. First, after inducing irreversible changes in the  $I-V$  characteristics (i.e., increasing the voltage required for a given current), the trend is for the surface magnification to decrease. That is, the effective tip radius and emitting area increase relative to the prepulsing data. Second, the emission patterns change from the random lobes of emission (typical of as-fabricated single tips) to patterns showing compelling signs of crystallinity.

The decrease in the field-voltage proportionality factor (i.e., increased voltage required to extract a given current) as a result of pulsed current heating at elevated emission currents is evident by the increase in emitting area. Figure 6(a) is a micrograph of an as-fabricated single tip emitting  $1 \mu\text{A}$  after operation for 90 h at  $10 \mu\text{A}$ . The low frequency component of the current ( $<0.01 \text{ Hz}$ ) showed a bistable character with the total emission current fluctuating between 1.0 and  $2.0 \mu\text{A}$  at constant voltage. Figure 6(b) is a micrograph of the tip emitting  $1 \mu\text{A}$ . Apparently atomic level changes occurring on the tip surface, which lead to bistable changes in the emission current, can also induce significant changes in the electron emission spatial distribution, particularly when

the emitting areas are quite small. From the FN data, the calculated emitting area in Fig. 6 is  $\sim 100 \text{ \AA}^2$ . However, after pulsed heating and the induced decrease in the field-voltage proportionality factor, single atomic or molecular events have a much reduced influence on the pattern due to the increase in emitting area.

Figures 7(a) and 7(b) are emission patterns of a cathode that, in its as-fabricated state, showed changes similar to those in Figs. 6(a) and 6(b). Pulsed treatment at 2.2 mA resulted in a significant increase ( $\sim 2\times$ ) in operational voltage for a given current and a large increase in emitting area from 100 to  $\sim 5 \times 10^4 \text{ \AA}^2$ . Again, the pattern is modified by single atomic scale events; however, now the change occurs in only a small region of the entire pattern, as seen within the encircled area showing the principle difference between patterns 7(a) and 7(b). Such pattern changes are similar to those observed with flash annealed etched wire tips, which typically have emitting areas greater than  $10^6 \text{ \AA}^2$ .

Further evidence supporting the observation of thermally activated field assisted surface self-diffusion is given by the FEEM images shown in Figs. 8–10. These figures show a series of FEEM patterns before and after emission current pulsed heating. Figure 8(a) is the electron pattern before pulsing. Figure 8(b) is the pattern after pulsing at  $700 \mu\text{A}$  ( $t_{\text{on}}=1.8 \text{ s}$ ) until no further significant changes in the  $I-V$  characteristics were observed after several hours of pulsing. Figures 8(a) and 8(b) correspond to the  $I-V$  data shown in,

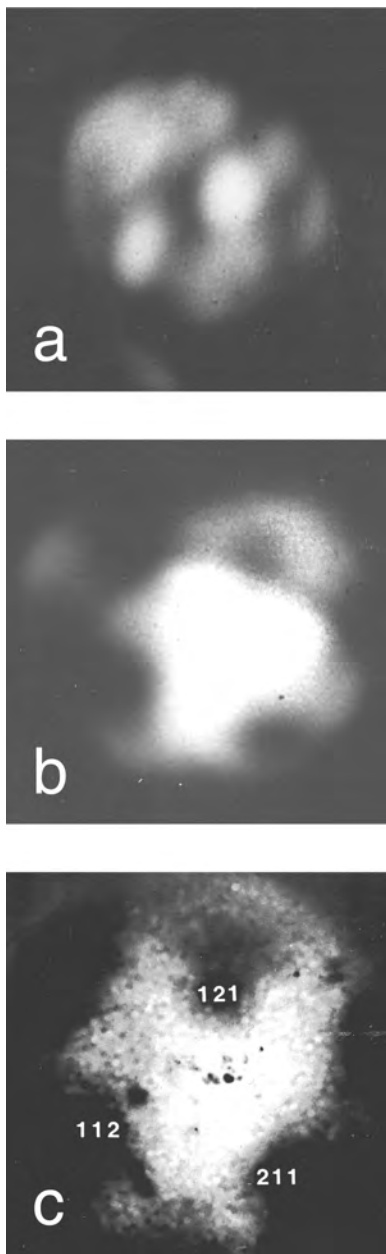


FIG. 8. (a) Emission pattern of an as-fabricated single tip cathode ( $I = 1 \mu\text{A}$ ,  $V = 114 \text{ V}$ ). (b) Pattern following pulsing at  $700 \mu\text{A}$  ( $I = 1 \mu\text{A}$ ,  $V = 133 \text{ V}$ ). (c) Pattern of a  $W\langle 111 \rangle$  single crystal etched wire tip ( $I = 1.5 \mu\text{A}$ ,  $V = 8000 \text{ V}$ ). Cathode No. 39J-514F-40B.

respectively, curves A and C of Figs. 1 and 2. The pattern in Fig. 8(a) is again very typical of as-fabricated emitter tips; one to several lobes of emission having no apparent symmetry. The pattern shown in Fig. 8(b) is quite different, however, as evidence of crystalline symmetry may be present. It is possible that the central bright region corresponds to a Mo  $\{111\}$  plane, due to the threefold symmetry, and that a portion of two  $\{110\}$  planes (at  $\sim 2$  and  $10$  o'clock) and three  $\{211\}$  planes are visible in the pattern. For comparison, Fig. 8(c) is the FEEM pattern of a  $W\langle 111 \rangle$  etched-wire single crystal tip, with the  $\{211\}$  type planes labeled.

Figure 9 shows not uncommon changes in the emission

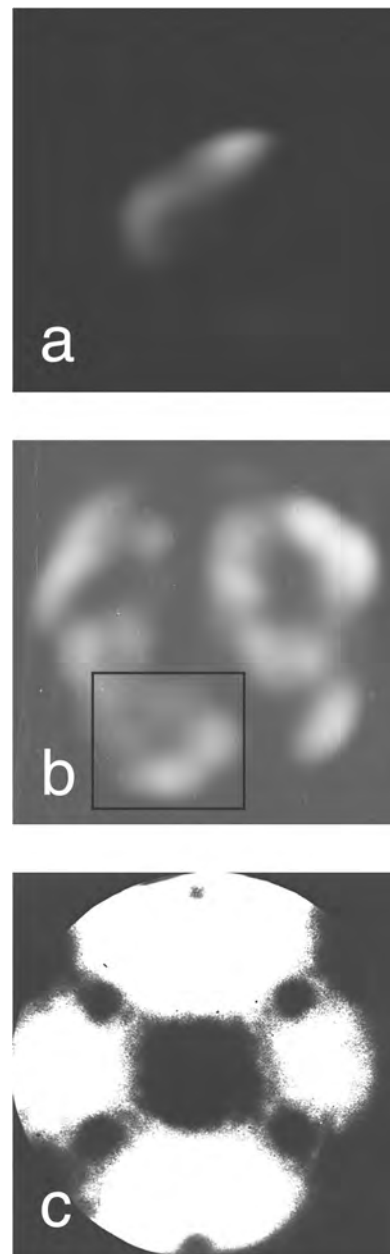


FIG. 9. (a) Pattern of an as-fabricated single tip cathode ( $I = 1 \mu\text{A}$ ,  $V = 116 \text{ V}$ ). (b) Pattern following pulsing at  $2.5 \text{ mA}$  ( $t_{\text{on}} = 10 \text{ s}$ ) ( $I = 1 \mu\text{A}$ ,  $V = 185 \text{ V}$ ). (c) Pattern of a  $W\langle 110 \rangle$  etched wire tip. Cathode No. 39J+510F-25C.

pattern after pulsing to emission currents exceeding  $\sim 1 \text{ mA}$  for seconds of ontime. Figure 9(a) is the emission pattern of the as-fabricated emitter tip and Fig. 9(b) is the pattern after pulsing at  $2.5 \text{ mA}$ . Figure 9(b) may show emission from multiple grains, similar to emission patterns from multiple single crystal whiskers.<sup>16</sup> It is likely that a  $\langle 110 \rangle$  grain is visible at 7 o'clock in the emission pattern. For reference, Fig. 9(c) is the FEEM pattern of a very clean  $W\langle 110 \rangle$  etched wire tip surface.

Figure 10 is a series of micrographs in which rhodium was deposited on the surface of the cathode. Figure 10(a) is the as-fabricated tip following normal operation at  $6 \mu\text{A}$  for

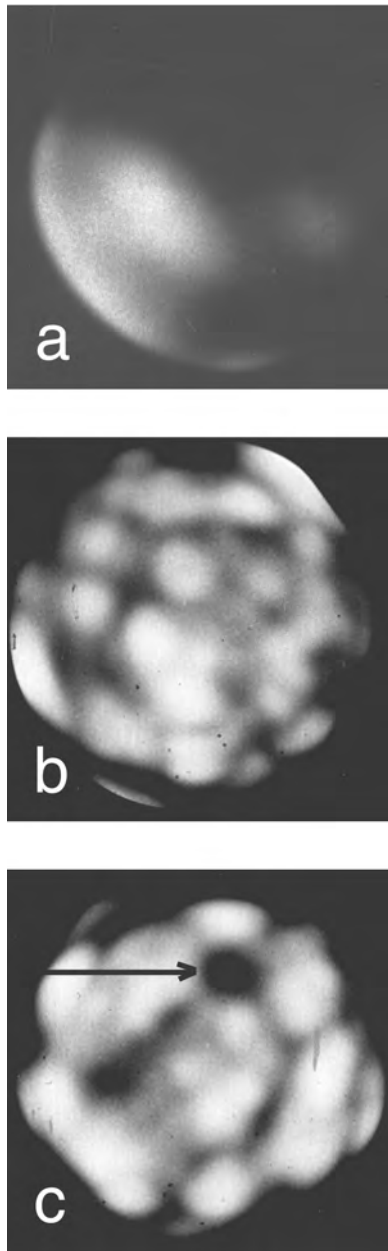


FIG. 10. (a) Emission pattern of an as-fabricated cathode. (b) Pattern following *in situ* deposition of rhodium. (c) Pattern following current pulsing at 1 mA. Cathode No. 39J+163F-1K.

24 h, again the typical lobe(s) of emission are visible and no symmetry is evident. Figure 10(b) shows this tip following the *in situ* deposition of rhodium from a rhodium wrapped W coil. Figure 10(c) shows the cathode after current pulsing at 1 mA ( $t_{\text{on}}=0.37$  s). The dark circular region, between 1 and 2 o'clock in the image, appears to be a Rh {100} plane that is slightly misaligned with the tip axis.

#### D. Emitter tip temperature

Emitter tip temperatures achieved by electron emission current heating are difficult to quantify, particularly because the detailed geometrical structure of the microfabricated emitter tips is not well known. Swanson *et al.* performed an

elegant set of such experiments on etched wire tungsten field emitters to determine the inversion temperature for the Nottingham heating and cooling domains.<sup>17</sup> Lacking such data in the present experiments, we can make only rough estimates.

If we assume an average tip radius of 200 Å, typical of our microfabricated tips, the *average* current density emitted from the apex region of the tip, with a current of 1 mA, is approximately  $10^8$  A/cm<sup>2</sup>. This is roughly the current density required to observe significant joule heating of conventional tungsten field emitter tips.<sup>11</sup> In particular, the corresponding current of  $\sim 1$  mA should be close to that required to stimulate significant thermal-field surface self-diffusion with our microfabricated cathodes.<sup>8</sup>

The field emission micrographs show evidence of surface recrystallization after a few seconds of operation at current levels of  $\sim 1$  mA. If we make the assumption that this implies the diffusing surface atoms have a mean square displacement on the order of the emitting area  $A_e$  in a time interval of  $\sim 1$  s, the diffusivity  $D$  is  $\sim A_e/1 \text{ s} = 10^4 \text{ Å}^2/\text{s}$ . From mass transfer data available for tungsten emitter tips, this surface diffusivity corresponds to a temperature of  $\sim 1000$  °C.<sup>18</sup> To estimate the temperature for molybdenum tips, we scale by the ratio of the melting points, yielding an estimated temperature for molybdenum of  $\sim 800$  °C. This is not unreasonable because recrystallization becomes rapid at temperatures approaching  $\sim 1/3$  the melting point of the material.<sup>19</sup> When molybdenum is heated to 800 °C in vacuum many common surface contaminants, including molybdenum oxides, can be removed from the surface.<sup>20,21</sup>

#### IV. SUMMARY AND CONCLUSIONS

Microfabricated field emitter cold cathodes were pulsed to current levels of 3.5 mA. At currents of approximately 200  $\mu\text{A}$ , a *reversible* change in the cathode's  $I$ - $V$  characteristic is observed that is consistent with the thermal desorption of weakly bound surface adsorbates, such as hydrogen, arriving from residual gas atmosphere. For current levels exceeding approximately 400  $\mu\text{A}$ , and often approaching 1–3 mA, *irreversible* changes in the  $I$ - $V$  characteristics are observed. These changes are consistent with smoothing of the tip surface via thermally activated field assisted surface self-diffusion. Preliminary field ion imaging studies of the cathodes also support this conclusion. The result of surface self-diffusion is a significant increase in emitting area on the tip surface, a decrease in emission current noise, and surface recrystallization.

Microfabricated cathode self-heating provides a technique for *in situ* emitter tip cleaning and shaping. In addition, this field forming technique could allow for the formation of oriented overgrowths on the tip surface. For many single-tip applications, such a technique is practical. Pulsed heating could also be used to enhance emission uniformity between tips in an array; however, there can be a limit to its usefulness if the total currents required to simultaneously process multiple tips are limited by device characteristics, such as the use of integral resistors in series with the tips.

## ACKNOWLEDGMENTS

The authors thank N. W. Parker, A. D. Brodie, E. Yin, F. Tsai, and G. Guo of Ion Diagnostics Inc., Santa Clara, CA, for supporting our research efforts which led to this work. The authors acknowledge useful discussions with R. A. Olson of Los Alamos National Laboratory and F. Charbonnier of the Linfield Research Institute and the support of SRI's Vacuum Microelectronics Staff: S. L. Shepherd, D. A. Thibert, and M. Simkins. This research was supported by Contract No. NAS3-96072, DARPA High Definition Systems program, funded through the NASA John H. Glenn Research Center, Lewis Field.

<sup>1</sup>P. R. Schwoebel and I. Brodie, *J. Vac. Sci. Technol. B* **13**, 1391 (1995).

<sup>2</sup>See, for example, E. E. Martin, J. K. Trolan, and W. P. Dyke, *Phys. Rev.* **31**, 782 (1959); W. P. Dyke, F. M. Charbonnier, R. W. Strayer, R. L. Floyd, J. P. Barbour, and J. K. Trolan, *ibid.* **31**, 790 (1959).

<sup>3</sup>See, for example, T. Kamasaki, T. Yoshida, T. Matsuda, N. Osakabe, A. Tonomura, I. Matsui, and K. Kitazawa, *Appl. Phys. Lett.* **76**, 1342 (2000).

<sup>4</sup>D. Alpert, D. Lee, E. M. Lyman, and H. E. Tomasche, *J. Appl. Phys.* **38**, 880 (1967).

<sup>5</sup>I. Brodie and C. A. Spindt, *Adv. Electron. Electron Phys.* **83**, 1 (1992).

<sup>6</sup>R. A. Olson, G. R. Condon, J. A. Panitz, and P. R. Schwoebel, *J. Appl. Phys.* **87**, 2031 (2000).

<sup>7</sup>H.-D. Beckey, *Field Ionization Mass Spectrometry* (Pergamon, Braunschweig, 1971).

<sup>8</sup>P. R. Schwoebel, R. A. Olson, J. A. Panitz, and A. D. Brodie, *J. Vac. Sci. Technol. B* **18**, 2579 (2000).

<sup>9</sup>C. A. Spindt, U.S. Patent No. 5 064 396 (Nov. 1991).

<sup>10</sup>P. C. Bettler and F. M. Charbonnier, *Phys. Rev.* **119**, 85 (1960).

<sup>11</sup>W. P. Dyke, J. K. Trolan, E. E. Martin, and J. P. Barbour, *Phys. Rev.* **91**, 1043 (1953); W. W. Dolan, W. P. Dyke, and J. K. Trolan, *ibid.* **91**, 1054 (1953).

<sup>12</sup>H. B. Michaelson, *J. Appl. Phys.* **48**, 7729 (1992).

<sup>13</sup>E. Chranowski, *Acta Phys. Pol. A* **44**, 711 (1973).

<sup>14</sup>R. Gomer, R. Wortman, and R. Lundy, *J. Chem. Phys.* **26**, 1147 (1957).

<sup>15</sup>W. A. Mackie, T. Xie, J. E. Blackwood, S. C. Williams, and P. R. Davis, *J. Vac. Sci. Technol. B* **16**, 1215 (1998), and references therein.

<sup>16</sup>See, for example, R. Gomer, *Field Emission and Field Ionization* (Harvard, Cambridge, 1961).

<sup>17</sup>L. W. Swanson, L. C. Crouser, and F. M. Charbonnier, *Phys. Rev.* **151**, 327 (1966).

<sup>18</sup>H. P. Bonzel, *CRC Crit. Rev. Solid State Sci.* **6**, 171 (1976).

<sup>19</sup>C. S. Barrett, *Structure of Metals* (McGraw-Hill, New York, 1952).

<sup>20</sup>G. J. Dooley and T. W. Hass, *J. Vac. Sci. Technol.* **7**, S90 (1970).

<sup>21</sup>E. A. Gulbransen, K. F. Andrew, and F. A. Brassart, *J. Electrochem. Soc.* **110**, 952 (1963).